Production of strange particles and hypernuclei in nuclear reactions at a few GeV. New capabilities in the INCL intranuclear cascade model

Cite as: AIP Conference Proceedings **2130**, 040014 (2019); https://doi.org/10.1063/1.5118411
Published Online: 25 July 2019

J.-C. David, J. Hirtz, J. L. Rodriguez-Sanchez, A. Boudard, J. Cugnon, S. Leray, I. Leya, D. Mancusi, and G. Schnabel

Production of Strange Particles and Hypernuclei in Nuclear Reactions at a Few GeV. New Capabilities in the INCL Intranuclear Cascade Model.

J.-C. David[1,a)], J. Hirtz[1,2], J.L. Rodriguez-Sanchez[1,3,4], A. Boudard[1], J. Cugnon[5], S. Leray[1], I. Leya[2], D. Mancusi[6] and G. Schnabel[1]

[1]*IRFU, CEA, Université Paris-Saclay, F-91191, Gif-sur-Yvette, France*
[2]*Space Research and Planetary Sciences, Physics Institute, University of Bern, Sidlerstrasse 5, 3012 Bern, Switzerland*
[3]*Universidad de Santiago de Compostela, E-15782 Santiago de Compostela, Spain*
[4]*GSI-Helmholtzzentrum für Schwerionenforschung GmbH, D-64291 Darmstadt, Germany*
[5]*AGO department, University of Liège, allée du 6 août 19, bâtiment B5, B-4000 Liège, Belgium*
[6]*Den-Service d'étude des réacteurs et de mathématiques appliquées (SERMA), CEA, Université Paris-Saclay, F-91191, Gif-sur-Yvette, France*

[a)]Corresponding author: jean-christophe.david@cea.fr

Abstract. Motivated by a renewed interest in studies of hypernuclei, the strangeness degree of freedom was implemented in the intranuclear cascade model INCL. This model takes care of the first stage of reactions between a nucleon (or a light cluster) and a nucleus at energies from a few tens of MeV up to a few GeV. After emission of fast particles, a hot remnant nucleus is produced and another model, combined to INCL, handles the de-excitation (the Abla model in our case). The main ingredients will be discussed and we will compare the results to experimental data. The experimental kaon spectra for different target elements and at different energies agree reasonable well with the model predictions. The main remaining discrepancies are analysed and will be explained.

INTRODUCTION

On the one hand, hypernuclei provide a suitable laboratory to study YN and YY interactions. While strange nuclei are known for a long time, new experiments, either in progress or planned, in several worldwide facilities (JPARC, MAMI, JLab, GSI, FAIR, ...), makes the topic more and more attractive and exciting. Obviously the light hypernuclei have been studied more extensively than the heaviest ones, but still some questions remain. As examples, we can cite in particular the ${}^{3}_{\Lambda}$H lifetime, which is shorter than the lifetime of the free Λ, and the Charge Symmetry Breaking observed in the Λ binding energy of the two mirror nuclei ${}^{4}_{\Lambda}$H and ${}^{4}_{\Lambda}$He. The heavier hypernuclei are also interesting objects to study. They are ideal to study the behavior of hyperons in nuclear matter and, beyond, to get information on the role of the Λ particles in neutron stars.

On the other hand, there is a nuclear reaction code, called INCL (Liège IntraNuclear Cascade), which treats reactions between light particles and atomic nuclei with incident energies from ~100 MeV up to a few GeV. More precisely, this code handles the first stage of the reaction, leading to an excited nuclear remnant. The de-excitation is usually treated by Abla, a code often combined to INCL to simulate the entire reaction. INCL, combined to Abla, is known as a reliable code-combination in the non-strange sector for energies up to 2-3 GeV [1] and, after 2010 with implementation of the multiple pion emission, up to ~15 GeV [2, 3].

The renewed interest in hypernucleus studies and the sound bases of the model implemented in INCL were the motivations to add K's, Λ and Σ's as participant particles in INCL. Most important reactions involving these particles are also included. The de-excitation code Abla was also upgraded with the evaporation of Λ's and fission of hypernuclei (hyperfission). Below we give first the ingredients required to perform the calculations and, second,

The 13th International Conference on Hypernuclear and Strange Particle Physics
AIP Conf. Proc. 2130, 040014-1–040014-8; https://doi.org/10.1063/1.5118411
Published by AIP Publishing. 978-0-7354-1872-1/$30.00

we compare the obtained results to experimental data and to predictions from other model codes. We conclude this paper by summarizing the benchmarking of the code on strange particle emission and on hypernucleus production, with possible improvements.

More than twenty years ago, an INCL version including strange particles was already built. However, at that time, INCL was not as sophisticated as now, some elementary ingredients were only ill-known, and the computer capabilities forced to simplify some aspects (for more details, see [4]). Moreover, the code of this version was oriented to the antiproton-nucleus case and, unfortunately, is no more available.

INGREDIENTS

An intranuclear cascade is a series of collisions between hadrons. The main ingredients to simulate such collisions are the elementary cross sections (production, scattering, absorption), the particle momenta and charges in the output channels, the nuclear potential felt by all particles, and, possibly, their decay. Obviously, other aspects, like Pauli blocking, must be also taken into account. It must be stressed that in INCL the resonances are not considered as participant particles (except the $\Delta(1232)$); Only their decay products play a role. The reason is threefold. First, the half-lives are short compared to the time between two interactions, second, some resonances overlap and, third, the needed information (cross sections, etc.) are not well known, requiring additional hypotheses.

Cross Sections

Adding the four Kaons ($K^+, K^-, K^0, \bar{K}^0$), the Λ and the three Σ (Σ^-, Σ^0, Σ^+), implies more than 400 new channels, when isospin is considered. We list below the channels accounted for in INCL. The implementation was done in two steps (Table 1 and Table 2). The second step turned out to be necessary after implementation of the first step.

This short report is not the place to explain all details of how each reaction cross section was determined. This is described in a paper submitted for publication [5]. Here we only draw the attention to the difficulties to obtain all necessary information. As an example, the first set, defined in Table1, includes 382 isospin channels and therefore 382 cross section parametrizations. Only 17% of them can be obtained by using experimental data. Considering isospin symmetry at the initial and final states of some binary collisions, an extra 18% is obtained from relations between known and unknown cross sections. Still relying on isospin symmetry, but, this time, at each vertex of tree Feynman diagrams used within a hadron exchange model, 37% of the cross sections is determined by ratios between known and unknown cross sections. The remaining cross sections are based on models or hypotheses, more precisely, for the latter, assuming similarities when a hyperon (kaon) replaces a nucleon (pion). Obviously, the more hypotheses are needed, the more uncertainties are assigned to the reaction cross sections and benchmarking is the only way to know a posteriori the reliability of our model.

TABLE 1. List of the reactions involving strange particles in INCL. First set.

NN	→	NΛK	πN	→	ΛK	$\bar{K}$N	→	$\bar{K}$N	KN	→	KN
	→	NΣK		→	ΣK		→	Λπ		→	KNπ
	→	NΛKπ		→	ΛKπ		→	Σπ		→	KN$\pi\pi$
	→	NΣKπ		→	ΣKπ		→	$\bar{K}$Nπ	NΛ	→	NΛ
	→	NΛK$\pi\pi$		→	ΛK$\pi\pi$		→	Λ$\pi\pi$		→	NΣ
	→	NΣK$\pi\pi$		→	ΣK$\pi\pi$		→	Σ$\pi\pi$	NΣ	→	NΣ
	→	NNK$\bar{K}$		→	NK$\bar{K}$		→	$\bar{K}$N$\pi\pi$		→	NΛ

TABLE 2. List of the reactions involving strange particles in INCL. Second set. "X" stands for all associated particles.

ΔN	→	NΛK	NN	→	K + X
	→	NΣK			
	→	ΔΛK	πN	→	K + X
	→	ΔΣK			
	→	NNK$\bar{K}$			

Final State Characteristics

Once a reaction between two hadrons in the nucleus is chosen, charges and momenta of the particles in the final state must be defined. Concerning the charges, Clebsch Gordan coefficients are used as far as possible if two or more particles are involved. When the number of particles increases, additional models are sometimes needed to remove ambiguities. The reader will find more details in [2]. Otherwise, as in the case of the inclusive reactions listed in the second column of Table 2, results of other codes are used to determine the number and type of particles emitted. Momenta are taken from double differential cross sections, in case measurements exist, or by assuming isotropy or considering phase-space distribution. Here again, the reliability of our approach may differ from channel to channel.

Average Nuclear Potentials and Decays

While the potential is quite well known for the Λ, the K^+ potential is known to be slightly repulsive and the K^- potential strongly attractive. For Σ's the potential seems to be repulsive, but this is still under debate. For K^0 and $\bar{K}^0$, the same potentials as for K^+ and K^-, respectively, were assumed, but corrected to Coulomb force. The values used in this study are: V_Λ=-28 MeV, V_Σ = 16 MeV, V_{K^+} = 25 MeV, V_{K^-} = -60 MeV, V_{K^0} = 25 MeV, $V_{\bar{K}^0}$ = -50 MeV. The latest value implemented in INCL for V_Λ is actually mass dependent. However, the results presented here were performed with the value of -28 MeV, which is very close to the new $V_\Lambda(A)$ for the light and medium mass nuclei. Note that, the potential play a role mainly at low energies.

With half-lives around 10^{-8}s or 10^{-10}s, no strange particle decays during the cascade, except the Σ^0 (10^{-20}s). The latter point is important for Λ and Λ-hypernucleus production rates. Once emitted, obviously, all strange particles will ultimately decay.

RESULTS

Comparisons to experimental data and other models are the only way to test the reliability of a model and to try to understand remaining deficiencies. Most of the measured data in this domain are related to the K^+ production. However, some other data exist and were used to benchmark this first version of INCL considering strangeness. Below, plots showing the production of K^+, K^-, K^0, Λ and hypernucleus are shown and analyzed.

K^+ production

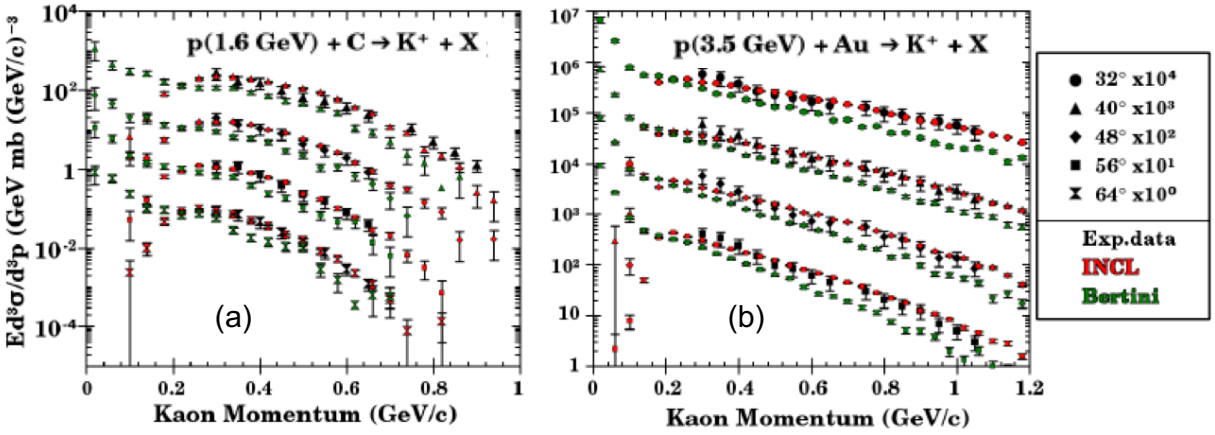

FIGURE 1. Invariant production cross sections of K^+ for inclusive proton-carbon collisions at 1.6 GeV (a) and proton-gold collisions at 3.5 GeV (b) as a function of laboratory momentum. Experimental data (black) are from [6]. Also shown are results from two models, Bertini [7] (green) and INCL (red).

Most of the time, the production of K^+ is well described by INCL. As an example we show two plots displaying the invariant production cross sections for five different angles of K^+ emission measured by the KaoS collaboration

for two different systems (Fig. 1); either by 1.6 GeV protons on a light target (carbon - (a)) or by 3.5 GeV protons on a heavy target (gold - (b)). The results of INCL match very well the experimental data. We also plotted the results from the Bertini model [7] implemented in the particle transport code Geant4 (like INCL). The INCL model is more than competitive. The difference between both models at low K^+ momenta is due to the different K^+ potential values.

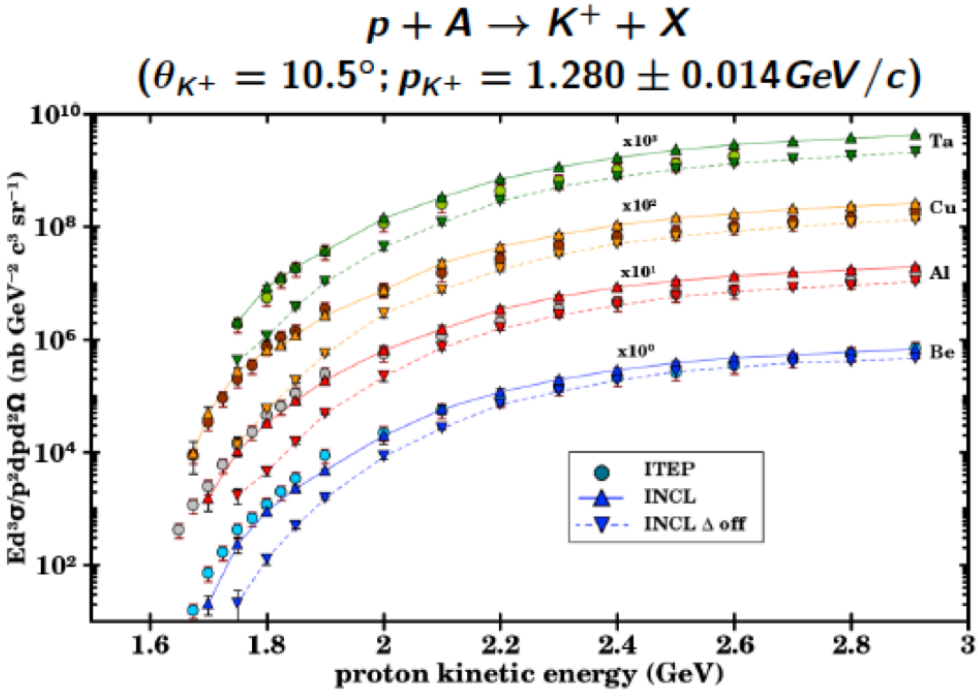

FIGURE 2. Invariant production cross sections of K^+ emitted with a momentum of 1.28±0.014 GeV/c at an angle of 10.5° for four targets as a function of proton projectile energy. Experimental data are from [8] (circles) and are compared to INCL with (up-oriented triangles) and without (down-oriented triangles) Δ-induced Kaon production.

Figure 2 depicts the production of K^+ as a function of proton projectile energy from threshold up to 2.9 GeV for four different targets. The motivation is to study the influence of the Δ on the production. K^+ are detected in a small specific phase-space, but the conclusions are rather universal. First, Δ's play an important role in K^+ production, especially at low energies and, second, INCL reproduces the data from ITEP. Going deeper in the analysis, we can see that INCL slightly overestimates the production with increasing proton energy. This is probably related to the parametrizations used for the Δ-induced Kaon production [9], where the authors already observed a discrepancy for the $\Delta N \rightarrow NYK$ reactions beyond 200 MeV. This is a potential topic to improve.

INCL can also handle heavier projectiles than protons. In Fig. 3(a) we plotted the results obtained for the reaction d(2.1 A.GeV)+^{208}Pb. The conclusions are the same as for proton projectiles (see Fig. 1), i.e., INCL matches well the LBL data [10]. At low kaon momentum experimental are missing; there existence would help to test the kaon potential.

In Fig. 2 we observed that K^+ production in the forward direction was rather well described for a given momentum and with respect to the proton projectile energy. In Fig. 3(b) we test the momentum spectrum, still in the forward direction. At low momenta the three models, INCL, LAQGSM [11] and Bertini fit well the experimental data. At higher momenta, INCL and LAQGSM reproduce the ANKE data [12] while Bertini underestimates them. Beyond the experimental data, all models have different shapes. Figure 2 implies that INCL would overestimate the cross section displayed in Fig. 3(b) for a K^+ momentum of 1.28 GeV/c by a factor of roughly 30%, which is compatible with the results of the Bertini code, but higher than LAQGSM. Δ-induced kaon production in INCL is probably, here again, overestimated. The same type of data in the entire momentum range would help to better understand the mechanisms involved.

All previous results are from reactions with projectile energies much lower than 10 GeV. In Fig. 4 (left) we test INCL at higher projectile energies, i.e., with 14.6 GeV/c protons [13]. INCL describes the spectra in rapidity for all

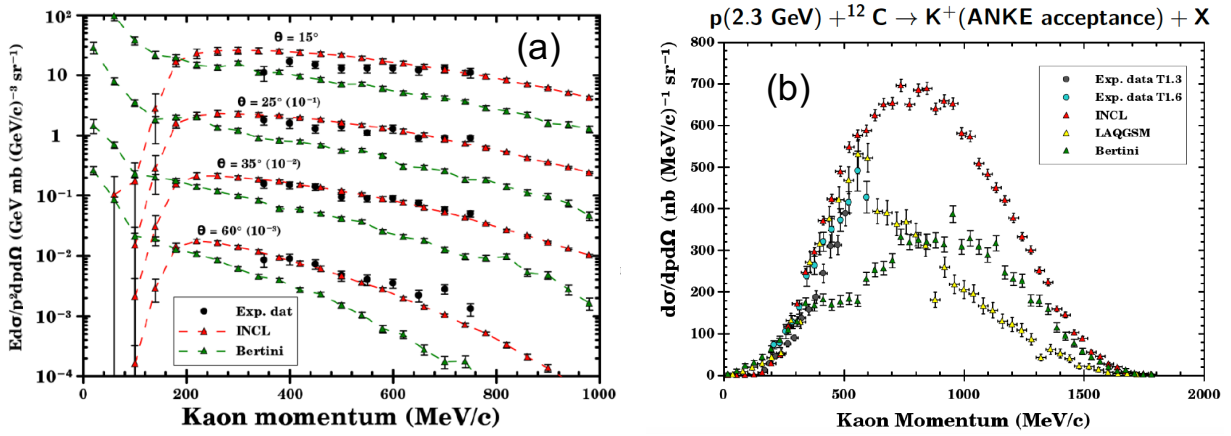

FIGURE 3. On the left part (a), invariant production cross sections of K^+ from the reaction d(2.1 A.GeV)+^{208}Pb as a function of the laboratory momentum. Experimental data (black bullets) measured at LBL [10] are compared to Bertini (green triangles) and INCL (red triangles). On the right part (b), K^+ momentum spectrum for the reaction p(2.3 GeV)+^{12}C. Experimental data (two types of bullets for two types of configuration) are from the ANKE experiment with an angular acceptance focussed in the forward direction [12]. Three calculation results (triangles) are plotted: INCL (red), LAQGSM [11] (yellow) and Bertini(green).

four targets well. The only deficiency is at high rapidity for the heaviest targets, where INCL slightly underestimates the data.

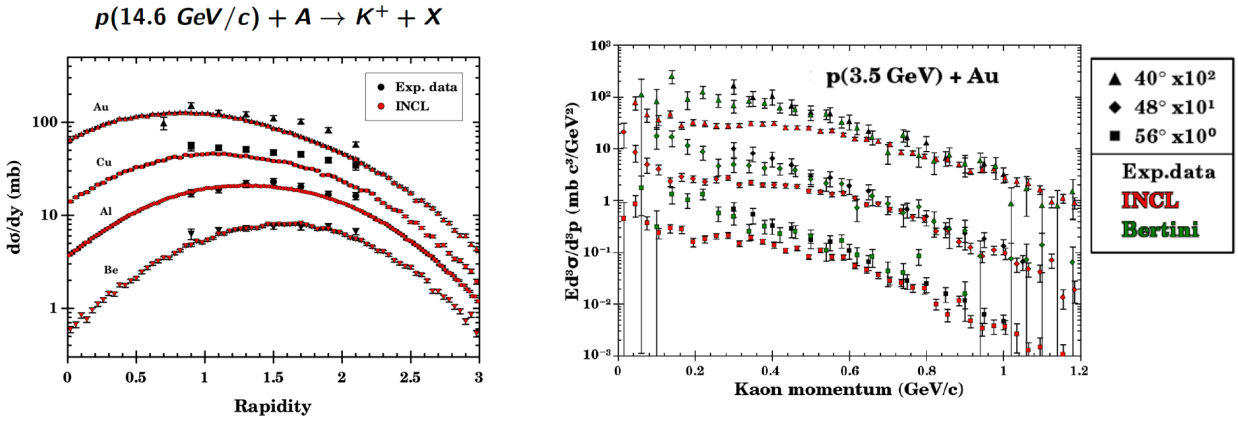

FIGURE 4. On the left, K^+ production in proton-induced reactions at 14.6 GeV/c on Be, Al, Cu, and Au targets as a function of the rapidity. Experimental data (black marks) are from [13] (E-802 Collaboration) and INCL results are shown in red. On the right, invariant production cross sections of K^- for inclusive proton-gold collisions at 3.5 GeV in function of the laboratory momentum. Experimental data (black) come from [6] and are also plotted two models, Bertini (green) and INCL (red).

K^- production

The conclusions for the K^- differ from the conclusions above for the K^+ (Fig. 4 - right part). The spectra are well reproduced except for low momenta. In this region the Bertini code gives better results, what seems to indicate that in INCL some production channels are missing, especially the $YN \rightarrow \bar{K}NN$. This corroborates the state made in [6], arguing that the role of strangeness exchange reactions was important in K^- production.

K_s^0 production

The only comparison between the model and experimental data and between different models for the K^0 is shown in Fig. 5 (left). INCL reproduces well the shape of the spectra, but overestimates the experimental data by about 40%. As for the K^+, the role of the Δ-induced production is maybe an explanation for the discrepancy, but there might be another reason. The total reaction cross section σ_{tot}^{pNb} used by HADES [14] for normalizing their experimental data is 848 mb, while INCL calculates a value of 1048 mb. A measurement of the total reaction cross section for the same system, but at a proton projectile energy of 1.2 GeV instead of 3.5 GeV, gave 1063±40 mb [15]. Therefore, some part of the overestimation is probably due to the normalization.

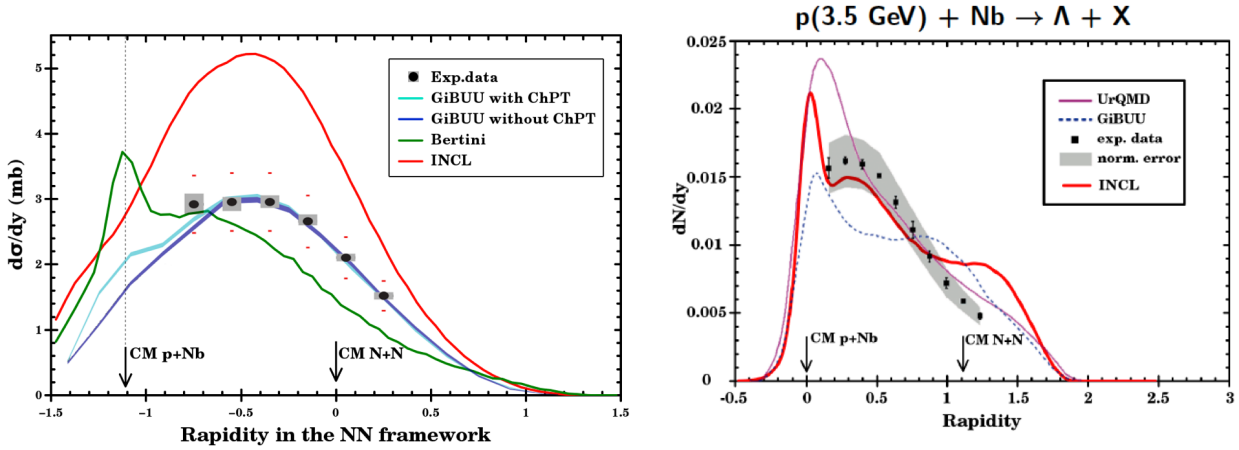

FIGURE 5. On the left, K_s^0 rapidity distribution in the nucleon-nucleon center-of-mass reference frame for p(3.5 GeV) + Nb collisions. HADES experimental data [14] are shown by filled circles. In addition several results are plotted: GiBUU transport model simulations with (cyan) and without (blue) the in-medium ChPT KN potential, Bertini (green) and INCL (red). The original plot is from [14]. On the right, Λ rapidity-density distribution for the reaction p(3.5 GeV) + Nb. The error bars show the systematic uncertainties. The gray-shaded band represents the uncertainty due of the absolute normalization. HADES data [16] are in black, UrQMD model predictions are in magenta, GiBUU model in dotted blue and INCL in red. The original plot is from [16].

Λ production

The production of hypernuclei is strongly connected to the production of Λ, since most of the observed hypernuclei are involving a Λ. Therefore, before studying the hypernucleus production, we tested our model for the production of Λ. Once again, experimental data are very scarce and we can only show one diagram. We compared the INCL results to the HADES rapidity spectrum for the reaction p(3.5 GeV) + Nb (Fig. 5 - right part), as well as to some other models. INCL matches rather well the HADES data [16], except for rapidities larger than 0.8. The *shoulder* seen with INCL,but not with the HADES data, also exists for the GiBUU model, but at lower rapidities. The UrQMD model does not exhibit such a behavior and is close to HADES, but misses strongly the two data points at low rapidity. The shape of the rapidity spectrum beyond 0.8 is possibly due to the low transverse momenta, but a careful study must be carried out to understand the differences between experimental data and model predictions.

Hypernucleus production

Considering hypernucleus production, we give two types of plots. The first (Fig. 6) shows the production of hypernuclei as a function of the mass target for cases in which one, and only one, K^+ is emitted by π^+-induced reactions (^{A}X(π^+,K^+)$^A_\Lambda$X). INCL fits very well the KEK experimental data. Only for the heaviest nuclei we see that INCL underestimates the KEK data. Remember that those calculations were performed with a constant nuclear potential for the Λ particle (V_Λ=-28 MeV). This deviation has been used to redefine the potential, assuming a dependence on the mass of the nucleus. The thus updated INCL model produces a perfect fit of the measurements (not shown here). This study has been accepted in Physical Review C. Another conclusion is the crucial role played by the de-excitation

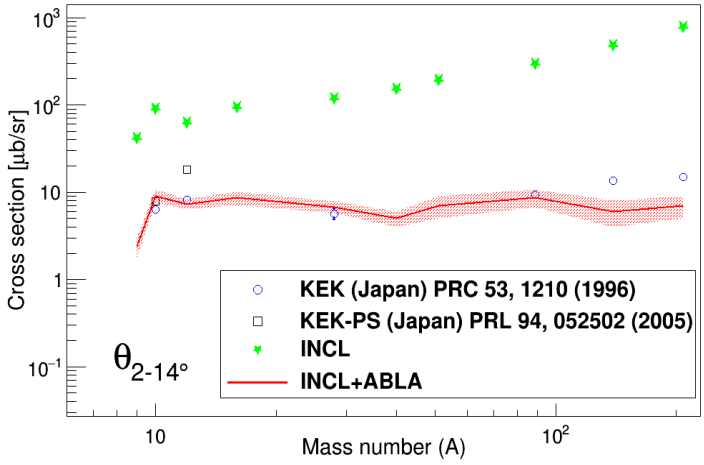

FIGURE 6. Hypernucleus production cross section in function of the mass target for ${}^{A}\mathrm{X}(\pi^{+},K^{+})^{A}_{\Lambda}\mathrm{X}$ reactions, with incident energies of 1.06 and 1.048 GeV/c. Experimental data are from [17](circles) and [18](squares). Are plotted INCL hyperremnant production (green stars) and INCL-Abla result (solid red line surrounded by a red band for the uncertainties).

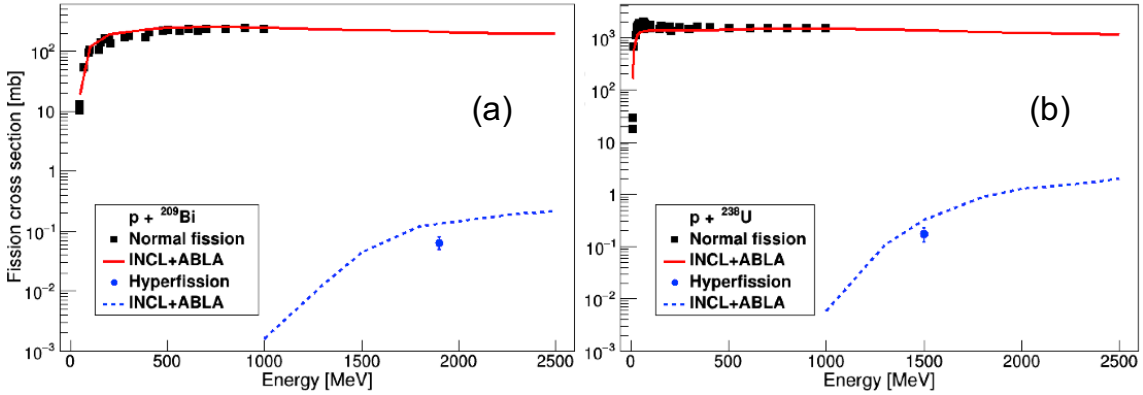

FIGURE 7. Fission and hyperfission cross sections in function of the proton projectile energy for two reactions: p+Bi (a) and p+U (b). Experimental data are from the web data base Exfor (https://www-nds.iaea.org/exfor/) for *normal* fission and from [19] (p+Bi) and [20] (p+U) for hyperfission. INCL results are in solid red lines for *normal* fission and in dotted-blue lines for hyperfission.

code, reducing the production rate by more than one order of magnitude compared to the rate at the end of the cascade. This latter result gives the probability that the Λ particle does not evaporate and the Abla code, upgraded on purpose, describes well the de-excitation of hypernuclei.

In Fig. 7 the fission of hypernuclei is tested. At the end of the intranuclear cascade, if the target is heavy enough, the remnant can undergo fission. This remnant can be a *normal* nucleus or a hypernucleus. For *normal* nuclei, we know that the combination INCL-Abla gives good results, as shown in Fig. 7. With the implementation of hyperfission in Abla, in particular by taking into account hyperenergy in the fission barrier height, we conclude that Abla is able to calculate a fission cross section very close to the rare experimental data, although hyperfission is four orders of magnitude less likely than *normal* fission.

CONCLUSION

The strange particles $K^{+}, K^{-}, K^{0}, \bar{\mathrm{K}}^{0}$, Λ, Σ^{-}, Σ^{0} and Σ^{+} are implemented into the intranuclear cascade code INCL. Since the de-excitation code Abla is usually combined to INCL for a full simulation of spallation reactions, Abla has been also upgraded by adding Λ evaporation and hyperfission. Results obtained by the codes, and especially

INCL, are very encouraging. Main mechanisms are incorporated and now it is time for improvements. Δ-induced strangeness production is probably overestimated when energy goes up and some strangeness exchange reactions must be added, like $\Lambda N \rightarrow \bar{K}NN$, to better reproduce K^- production. Other aspects must also be studied, like the momentum distribution of the emitted particles. However, the lack of experimental data to get better elementary ingredients and to benchmark carefully our model makes the task difficult.

REFERENCES

[1] S. Leray, J. C. David, M. Khandaker, G. Mank, A. Mengoni, N. Otsuka, D. Filges, F. Gallmeier, A. Konobeyev, and R. Michel, J. Korean Phys. Soc. **59**, 791–796 (2011).

[2] S. Pedoux and J. Cugnon, Nucl. Phys. A **866**, 16–36 (2011).

[3] D. Mancusi, S. L. Meo, N. Colonna, A. Boudard, M. A. Cortes-Giraldo, J. Cugnon, J.-C. David, S. Leray, J. Lerendegui-Marco, C. Massimi, and V. Vlachoudis, Eur. Phys. J. A **53**, p. 80 (2017).

[4] J. Cugnon, P. Deneye, and J. Vandermeulen, Phys. Rev. C **41**, p. 1701 (1990).

[5] J. Hirtz, J.-C. David, A. Boudard, J. Cugnon, S. Leray, I. Leya, and D. Mancusi, (submitted for publication).

[6] W. Scheinast (KaoS Collaboration), Phys. Rev. Lett. **96**, p. 072301 (2006).

[7] D. Wright and M. Kelsey, Nucl. Instr. and Meth. A **804**, 175–188 (2015).

[8] A. V. Akindinov, Y. T. Kiselev, A. N. Martem'yanov, V. I. Mikhailichenko, K. R. Mikhailov, S. A. Pozdnyakov, Y. V. Terekhov, M. M. Chumakov, and V. A. Sheinkman, Journal of Experimental and Theoretical Physics Letters **72**, 100–105 (2000).

[9] K. Tsushima, A. Sibirtsev, A. W. Thomas, and G. Q. Li, Phys. Rev. C **59**, p. 369 (1999).

[10] S. Schnetzer, R. M. Lombard, M.-C. Lemaire, E. Moeller, S. Nagamiya, G. Shapiro, H. Steiner, and I. Tanihata, Phys. Rev. C **40**, 640–653 (1989).

[11] N. Mokhov, K. Gudima, and S. Striganov., ArXiv:1409.1086[nucl-ex].

[12] M. Büscher, V. Koptev, M. Nekipelov, Z. Rudy, H. Ströher, Y. Valdau, S. Barsov, M. Hartmann, V. Hejny, V. Kleber, N. Lang, I. Lehmann, S. Mikirtychiants, and H. Ohm, Eur. Phys. J. A **22**, 301–317 (2004).

[13] T. Abbott (E-802 Collaboration), Phys. Rev. D **45**, 3906–3920 (1992).

[14] G. Agakishiev (HADES Collaboration), Phys. Rev. C **90**, p. 054906 (2014).

[15] C.-M. Herbach, D. Hilscher, U. Jahnke, V. G. Tishchenko, J. Galin, A. Letourneau, A. Peghaire, D. Filges, F. Goldenbaum, L. Pienkowski, W. U. Schroeder, and J. Toke, Nucl. Instr. and Meth. A **562**, 729–732 (2006).

[16] G. Agakishiev (HADES Collaboration), Eur. Phys. J. A **50**, p. 81 (2014).

[17] T. Hasegawa, O. Hashimoto, S. Homma, T. Miyachi, T. Nagae, M. Sekimoto, T. Shibata, H. Sakaguchi, T. Takahashi, K. Aoki, H. Noumi, H. Bhang, M. Youn, Y. Gavrilov, S. Ajimura, T. Kishimoto, A. Ohkusu, K. Maeda, R. Sawafta, and R. P. Redwine, Phys. Rev. C **53**, 1210–1220 (1996).

[18] P. K. Saha, T. Fukuda, W. Imoto, J. K. Ahn, S. Ajimura, K. Aoki, H. C. Bhang, H. Fujioka, H. Hotchi, J. I. Hwang, T. Itabashi, B. H. Kang, H. D. Kim, M. J. Kim, T. Kishimoto, A. Krutenkova, T. Maruta, Y. Miura, K. Miwa, T. Nagae, H. Noumi, H. Outa, T. Ohtaki, A. Sakaguchi, Y. Sato, M. Sekimoto, Y. Shimizu, H. Tamura, K. Tanida, A. Toyoda, M. Ukai, and H. J. Yim, Phys. Rev. Lett. **94**, p. 052502 (2005).

[19] P. Kulessa, Z. Rudy, M. Hartmann, K. Pysz, B. Kamys, I. Zychor, H. Ohm, L. Jarczyk, A. Strzałkowski, W. Cassing, H. Hodde, W. Borgs, H. Koch, R. Maier, D. Prasuhn, M. Matoba, and O. Schult, Physics Letters B **427**, 403 – 408 (1998).

[20] H. Ohm, T. Hermes, W. Borgs, H. R. Koch, R. Maier, D. Prasuhn, H. J. Stein, O. W. B. Schult, K. Pysz, Z. Rudy, L. Jarczyk, B. Kamys, P. Kulessa, A. Strzalkowski, W. Cassing, Y. Uozumi, and I. Zychor, Phys. Rev. C **55**, 3062–3065 (1997).